cosmetics

MDPI

Article

Antifungal Activity and Safety of *Physalis angulata* Extract, Its Fraction, and Their Nanoemulsions as Candidate Cosmetic Ingredients: A Preliminary *In Vitro* Study

Camila Cristina Baccetti Medeiros [1], Rodrigo Sorrechia [1], Maria Leonor Beneli Donadon [1], Winner Duque Rodrigues [1], André Gonzaga dos Santos [1], Jonatas Duarte Lobato [1], Marlus Chorilli [1], Ana Luísa Rodriguez Gini [1], Pamela Souza Tada da Cunha [1], Cauê Benito Scarim [1], Fabiano Guimarães Silva [2], Ana Helena Januário [3], Ana Melero [4] and Rosemeire Cristina Linhari Rodrigues Pietro [1,*]

[1] School of Pharmaceutical Sciences, São Paulo State University "Julio de Mesquita Filho"—(UNESP), Araraquara 14800-903, SP, Brazil; camila.medeiros@unesp.br (C.C.B.M.)
[2] Department of Biology, Federal Institute of Education, Science and Technology, Rio Verde 74001-970, GO, Brazil
[3] Department of Chemistry, University of Franca, Franca 14401-135, SP, Brazil
[4] Faculty of Pharmacy, University of Valencia, 46010 Valencia, Spain
* Correspondence: rosemeire.pietro@unesp.br

Abstract

Physalis angulata L. is a source of lipophilic bioactive metabolites of interest for cosmetic research, but the antifungal behavior of its fractions in nanoemulsions remains poorly characterized. This study evaluated the antioxidant, antifungal, irritant, and cytotoxic activity of a chloroform extract (E) and a hexane–ethyl acetate (6:4) fraction (F) from *P. angulata*, and their nanoemulsions (NE-E, NE-F), using HPLC-UV, DPPH, microdilution, HET-CAM and HaCaT assays. HPLC-UV showed major peaks at 39–41 min, predominant in F. E showed moderate antioxidant activity (EC_{50} = 415 µg/mL), while F showed limited activity. F was active against all six microorganisms tested (*T. rubrum*, *T. mentagrophytes*, *M. canis*, *C. albicans*, *C. krusei*, *C. parapsilosis*), most potently against *M. canis* (MIC = 0.07 mg/mL). NE-F retained reduced activity against the dermatophytes but not against *Candida.* Samples showed no HET-CAM irritant effect. In HaCaT cells, NE-F showed an IC_{50} of 173.1 µg/mL; its MIC against *M. canis* (310 µg/mL) exceeded this value, indicating a limited cellular safety margin. The nanoemulsions remained in the nanometric range over 30 days, although NE-F showed a transient increase in PDI on Day 7. These results demonstrate the antifungal potential of fraction F and show that nanoemulsification partially preserved dermatophyte activity, supporting further investigation of F as a candidate cosmetic ingredient.

Keywords: *Physalis angulata*; nanoemulsion; antifungal activity

Check for updates

Academic Editor: Enzo Berardesca

Received: 31 July 2026
Revised: 15 October 2026
Accepted: 16 October 2026
Published: 20 October 2026

Copyright: © 2026 by the authors. Licensee MDPI, Basel, Switzerland. This article is an open access article distributed under the terms and conditions of the Creative Commons Attribution (CC BY) license.

1. Introduction

The growing interest in natural ingredients has driven the investigation of plant-derived materials as sources of bioactive compounds for the development of topical preparations. However, the chemical complexity of these materials can hinder their incorporation into preparations, especially when their constituents show low aqueous solubility or limited physicochemical stability [1].

Nanoemulsions have been investigated in the pharmaceutical and cosmetic fields as systems capable of incorporating and dispersing lipophilic substances in aqueous-based formulations. The reduced droplet size and physicochemical characteristics of these

systems can favor the dispersion of plant-derived lipophilic constituents, broadening the possibilities for developing preparations containing these materials [2].

The antifungal activity of plant-derived constituents incorporated into this type of system is particularly relevant given the diversity of fungi associated with superficial infections, which affect a large proportion of the world population and include dermatophytes, frequently associated with dermatophytoses, and yeasts of the genus Candida, associated with superficial and opportunistic fungal infections in humans [3,4]. *Physalis angulata* L. (Solanaceae) is a species widely distributed in tropical and subtropical regions and recognized as a source of structurally diverse specialized metabolites. Studies with the species and its preparations have described different biological activities, including antimicrobial, antifungal, and anti-inflammatory effects [5–8]. *P. angulata* is also known for the occurrence of withanolides and physalins, steroidal metabolites to which biological activities have been associated in studies conducted with plant preparations and isolated compounds [8,9]. Withanolides are C_{28} ergostane-type steroidal lactones, and physalins, highly oxygenated 16,24-cyclo-13,14-seco-steroids biogenetically related to them, are considered chemical markers of the genus *Physalis*; 78 physalins had been described in the genus by 2021, with anti-inflammatory, immunomodulatory, antimicrobial, antiparasitic, and anticancer activities reported [10]. Physalins obtained from *P. angulata* aerial parts, for instance, showed antimycobacterial activity [6,7].

The relevance of these constituents for dermatological and cosmetic products is supported by in vivo studies with topical preparations. Physalin E applied topically (0.125–0.5 mg/ear) reduced ear edema, myeloperoxidase activity, and TNF-α levels in murine models of dermatitis, with effects comparable to those of dexamethasone [11], and topical preparations of *P. angulata* in petrolatum (1:2 and 1:4, *w*/*w*) reduced IL-17 and IFN-γ expression in a murine psoriasis model [12]. However, the content of these metabolites in the raw material varies with plant organ, origin, and extraction procedure; validated methods for the quantification of major physalins in *P. angulata* have only recently been proposed [13], and reference doses for their use in cosmetic preparations have not yet been established.

Although preparations of *P. angulata* and its constituents have been investigated for different biological activities, the low aqueous solubility characteristic of its metabolites still limits their direct incorporation into aqueous-based formulations [2,10].

Accordingly, this study evaluated the antifungal activity of a chloroform extract (E) and a hexane–ethyl acetate (6:4) fraction (F), obtained from the aerial parts of *P. angulata*, as well as their respective nanoemulsions (NE-E and NE-F), against the dermatophytes *Microsporum canis*, *Trichophyton rubrum*, and *Trichophyton mentagrophytes* and the yeasts *Candida albicans*, *Candida krusei*, and *Candida parapsilosis*. The chromatographic profiles of E and F by HPLC-UV, antioxidant activity, physicochemical characteristics and physical stability of the nanoemulsions over 30 days, and irritant potential and in vitro cytotoxicity were also evaluated.

2. Materials and Methods

2.1. Plant Material and Extract Preparation

Dried aerial parts of *Physalis angulata* L., previously identified, were collected in Rio Verde, Goiás, Brazil, in May 2020, through an institutional partnership under the coordination of Prof. Fabiano Guimarães Silva (Federal Institute of Goiás, Rio Verde Campus), and are registered in the National System for the Management of Genetic Heritage and Associated Traditional Knowledge (SisGen—registration no. AD73F75). The plant material was dried in a forced-air circulation oven (model 315 SE, Fanem, São Paulo, SP, Brazil) at 38 °C and ground in a knife mill (model TE-814, Tecnal, Piracicaba, SP, Brazil).

The ground plant material (233 g) was subjected to maceration with chloroform (Synth, Diadema, SP, Brazil) at a plant-to-solvent ratio of 1:20 (*w*/*v*; 50 g/L) for 72 h at room temperature, protected from light and without agitation. The process was repeated twice with solvent renewal. The extracts were combined, filtered, and concentrated using a rotary evaporator (Model 804, Fisatom, São Paulo, SP, Brazil) at 40 °C and 80 rpm, then further dried under a fume hood until a constant weight was obtained [5,7].

The crude extract obtained was designated as extract (E). The extraction yield was determined gravimetrically based on the ratio between the mass of the dried extract and the mass of plant material used, as commonly described for plant extraction procedures [8,14], according to the equation: Yield (%) = $(m_E/m_P) \times 100$, where mE is the mass (g) of dried extract and mP is the mass (g) of dried plant material used.

2.2. Chromatographic Partitioning

The chloroform extract was fractionated by column chromatography (25 × 6 cm) packed with silica gel 60 (70–230 mesh, Merck, Darmstadt, Germany), previously dried at 110 °C for 60 min and used to fill two-thirds of the column height. The column was conditioned with hexane: ethyl acetate (9:1) in a volume equal to its dead volume, calculated as $Vm = \pi \times R^2 \times h \times 0.65$, where R is the column radius (cm) and h is the height occupied by the silica (cm). The extract (3.00 g) was adsorbed onto 2 g of silica with a few drops of chloroform and applied to the top of the column. Elution was performed with solvents of increasing polarity, 200 mL each: hexane: ethyl acetate (9:1, 7:3, 6:4, 3:7) (Synth, Diadema, SP, Brazil; LS Chemicals, Mumbai, Maharashtra, India), followed by ethyl acetate, and finally methanol (Synth, Diadema, SP, Brazil) [7]. The resulting fractions were concentrated using a rotary evaporator and stored under refrigeration (model DC35A, Electrolux do Brasil, Curitiba, PR, Brazil) (4 °C), protected from light until further use [15].

For subsequent assays, the crude extract (E) and the fraction eluted with hexane: ethyl acetate (6:4) (F) were selected [15,16].

2.3. Phytochemical Analysis (HPLC-UV)

Samples E and F were subjected to high-performance liquid chromatography (HPLC) analysis to obtain the chromatographic profile of *P. angulata* constituents, based on previously reported studies [7].

Both samples were prepared at a concentration of 2 mg/mL in 95% methanol (JT Baker, Center Valley, PA, USA), sonicated until fully dissolved, purified using SEP Pak RP-18 cartridges (Waters, Milford, MA, USA), and filtered through 0.22 µm membranes (Whatman, Maidstone, Kent, UK).

The analyses were conducted using a UHPLC Dionex UltiMate 3000 system (Thermo Fisher Scientific Inc., Waltham, MA, USA) equipped with a C18 column (250 × 4.6 mm, Thermo Fisher Scientific Inc., Waltham, MA, USA), maintained at 25 °C. Elution was performed using a gradient system with water (phase A) and 100% methanol (phase B), ranging from 5% to 95% of phase B over 45 min, at a flow rate of 1.0 mL/min. Detection was carried out at wavelengths of 230, 250, 300, and 350 nm. The chromatograms obtained at 230 nm were selected for presentation and discussion in this study.

Peak areas were determined using Chromeleon 6.80 software (Thermo Fisher Scientific Inc., Waltham, MA, USA).

2.4. Antioxidant Activity Assessment (DPPH Assay)

The antioxidant activity of samples E and F was determined using the 1,1-diphenyl-2-picrylhydrazyl (DPPH) free radical scavenging method [17,18]. Aliquots of 1.0 mL of each sample, previously solubilized in methanol (Synth, Diadema, SP, Brazil) at increasing concentrations (0 to 357 µg/mL), were mixed with 2.5 mL of a 0.004% (*w*/*v*) methanolic

DPPH solution (Sigma-Aldrich, St. Louis, MO, USA). The mixture was homogenized and kept in the dark at room temperature for 30 min. Absorbance was measured at 515 nm using a spectrophotometer (Bel Photonics, Osasco, SP, Brazil), with the DPPH solution in methanol serving as the blank.

As positive controls, standard solutions of ascorbic acid, gallic acid, rutin, and quercetin (all from Sigma-Aldrich, St. Louis, MO, USA) were used in the concentration ranges of 0–6, 0–2, 0–57, and 0–7 μg/mL, respectively. The percentage of DPPH radical inhibition was calculated based on the mean absorbance of the samples and used to construct the analytical curve. From the linear regression equation, the EC_{50} (effective concentration of free radical inhibition) value was determined. All assays were performed in technical triplicate.

The linear regression equations (y = DPPH inhibition, %; x = concentration, μg/mL) and coefficients of determination were: extract E, y = 0.116x + 1.787 (R^2 = 0.960); gallic acid, y = 42.329x + 8.639 (R^2 = 0.940); ascorbic acid, y = 15.966x + 10.309 (R^2 = 0.961); quercetin, y = 10.561x + 7.902 (R^2 = 0.979); and rutin, y = 1.613x + 6.846 (R^2 = 0.926). Since the inhibition produced by E did not reach 50% within the tested range, its EC_{50} was estimated by extrapolation of the regression equation. For fraction F, 50% inhibition was not reached up to the highest concentration tested (357 μg/mL).

2.5. Nanoemulsion Formulation

Nanoemulsions were prepared based on previously reported nanoemulsion systems, with modifications [2]. Extract (E) and fraction (F) were incorporated into the formulations at a concentration of 5 mg/g (0.5% *w*/*w*), previously dissolved in the oil phase, yielding the nanoemulsions NE-E and NE-F, respectively. A blank nanoemulsion without active compounds was also prepared and designated as NE-B. The oil phase consisted of soybean phosphatidylcholine (Phospholipon 90, Lipoid, Ludwigshafen, Germany; 0.4% *w*/*w*; lipophilic surfactant)(0.4% *w*/*w*; lipophilic surfactant), medium-chain triglycerides (Labrafac Lipophile, Gattefossé, Saint-Priest, France; 1.8% *w*/*w*; oil), and polysorbate 80 (Sigma-Aldrich, St. Louis, MO, USA; 2.1% *w*/*w*; hydrophilic surfactant). The aqueous phase was composed of purified water (q.s. to 5 g).Both phases were heated to 70 °C, and the aqueous phase was slowly added to the oil phase under magnetic stirring (LGI-MSH-5 Basic, LGI Scientific, São Paulo, SP, Brazil) to form a pre-emulsion. This pre-emulsion was then sonicated using a probe sonicator (Q700, Qsonica, Newtown, CT, USA) for 5 min (1 min on, 30 s off, at 35% amplitude). The formulations were diluted with deionized water and characterized for mean droplet diameter, polydispersity index (PDI), and zeta potential by dynamic light scattering (DLS) using a Zetasizer Nano ZS (Malvern, Worcestershire, UK). All analyses were performed in technical triplicate. The formulations were stored under refrigeration (4 °C) and protected from light until use.

Particle size, PDI, and zeta potential data were expressed as mean ± standard deviation (SD). The effects of formulation and storage time on these physicochemical parameters were evaluated using two-way analysis of variance (ANOVA). When significant differences were detected, Dunnett's multiple-comparisons test was applied to compare each storage time point (Days 7 and 30) with Day 1 within the corresponding formulation. Differences were considered statistically significant at $p < 0.05$. Statistical analyses were performed using GraphPad Prism version 11 (GraphPad Software, Boston, MA, USA).

2.6. Antimicrobial Activity Assessment

Antifungal activity was evaluated by broth microdilution, following CLSI guidelines. For the dermatophytes (*M. canis*, *T. rubrum*, and *T. mentagrophytes*), the CLSI M38-A2 protocol [19] was used, with incubation at 28 °C for 7 days. For the yeasts (*C. albicans*, *C.*

krusei, and *C. parapsilosis*), the CLSI M27, 4th edition protocol was used, with incubation at 35 °C for 48 h [20]. The inoculum was standardized to 5×10^3 CFU/mL for dermatophytes and 2×10^4 CFU/mL for yeasts in 0.9% saline solution, using RPMI-1640 medium (Roswell Park Memorial Institute 1640 medium—Sigma-Aldrich, St. Louis, MO, USA) prepared according to the manufacturer's instructions. Amphotericin B (Ampho B; Sigma-Aldrich, St. Louis, MO, USA), used as the positive control, was prepared at 1.6 mg/mL in DMSO (Sigma-Aldrich, St. Louis, MO, USA) and diluted 1:25 at the time of use. The negative control consisted of 10% DMSO diluted in RPMI medium, without the addition of any active compound.

Five samples were tested: E, F, NE-E, NE-F, and NE-B (blank nanoemulsion, formulation control) against the six microorganisms evaluated. E and F were solubilized in 10% DMSO and diluted in RPMI medium to obtain a starting concentration of 5 mg/mL, while the nanoemulsions were applied directly. For the nanoemulsions, concentrations are expressed as the nominal content of E or F.

The assay was performed by broth microdilution in 96-well plates, with 1:1 serial dilution and a final volume of 100 µL per well. After inoculum addition, the plates were incubated in a refrigerated shaker incubator (model SL-221, Solab, Piracicaba, SP, Brazil) at 125 rpm, according to the temperature and time conditions described for each microbial group. The MIC reading was performed by checking the last well showing visible inhibition of microbial growth. The Minimum Fungicidal Concentration (MFC) was determined for all six microorganisms, by subculturing aliquots onto Sabouraud dextrose agar (SDA, Kasvi, Curitiba, PR, Brazil) after incubation and was defined by the absence of microbial growth.

To determine the Minimum Inhibitory Concentration (MIC), 20 µL of 0.01% resazurin solution (Sigma-Aldrich, St. Louis, MO, USA) was added as a viability indicator [21], and color change was assessed after 24 h for the dermatophytes and after 4 h for the yeasts, reflecting the faster growth of this group. MIC and MFC values were defined based on the mode of the independent triplicates, corresponding to the most recurrent concentration among replicates. As discrete endpoints obtained from a twofold serial-dilution scheme, MIC and MFC values were not subjected to parametric statistical analysis. Considering the inherent reproducibility of broth microdilution methods (±one twofold dilution), only differences greater than one dilution step (≥4-fold) between samples were interpreted as relevant.

2.7. Irritant Potential Assessment by HET-CAM

The HET-CAM assay was performed using fertilized Leghorn chicken eggs incubated for six days at 37.5 ± 0.5 °C and 55–65% relative humidity, following previously described procedures [22,23]. On the fourth day, embryonic viability was verified by transillumination, and an opening was made in the eggshell and sealed with Parafilm® (Bemis Company, Inc., now part of Amcor, Neenah, WI, USA). On the sixth day, 300 µL of each sample was applied directly onto the chorioallantoic membrane (CAM). E and F were solubilized in 1% DMSO for application; the nanoemulsions (NE-E, NE-F, NE-B) were applied directly. The DMSO concentration used (1%) was defined based on prior laboratory standardization, in which higher concentrations were shown to be cytotoxic to the chorioallantoic membrane. The samples evaluated included E, F, NE-E, NE-F, and NE-B, along with positive (0.1 M NaOH) and negative (0.9% NaCl) controls.

The CAM was observed under a digital microscope (Universal G600, model MS1329, Shenzhen, China) for 300 s, recording the onset times (s) of hemorrhage (H), lysis (L), and coagulation (C). The irritation score (IS) was calculated according to the equation $IS = [(301 - H)/300 \times 5] + [(301 - L)/300 \times 7] + [(301 - C)/300 \times 9]$, in which reactions not observed within 300 s were assigned a time of 300 s, and classified as follows: 0–0.9, (–)

no irritation; 1–4.9, (+) slight irritation; 5–8.9, (++) moderate irritation; 9–21, (+++) severe irritation [22,23]. Embryonic viability was monitored for up to 600 s after application. All experiments were performed in technical triplicate. Statistical comparisons between groups were conducted using one-way analysis of variance (ANOVA), followed by Tukey's test, with a significance level set at $p < 0.05$. Analyses were performed using GraphPad Prism 8.0.2 software (GraphPad Software Inc., San Diego, CA, USA).

2.8. In Vitro Cytotoxicity Assessment

Cytotoxicity was evaluated using the human keratinocyte cell line HaCaT, following previously described methods [24]. Cells were cultured in Dulbecco's Modified Eagle Medium (DMEM) supplemented with 10% fetal bovine serum (FBS) and 1% antibiotics, maintained at 37 °C and 5% CO_2. A total of 2×10^4 cells per well were seeded in 96-well plates and incubated for 24 h. Five samples were tested: E, F, NE-E, NE-F, and NE-B (control formulation).

After incubation, the medium was replaced with serum-free DMEM containing the test samples at concentrations of 100, 300, 600, 700, and 800 µg/mL. For the nanoemulsions, concentrations correspond to the nominal content of E or F. E and F were solubilized in 1% DMSO for this step; this concentration was defined based on prior laboratory standardization, which established that higher concentrations compromise cell viability. After 24 h of exposure, the wells were washed with PBS, and resazurin solution (0.1 mg/mL) was added as a cell viability indicator [25,26]. Fluorescence was measured after 3 h using a microplate reader (Synergy LX, BioTek/Agilent Technologies, Winooski, VT, USA) (λexcitation = 570 nm and λemission = 600 nm).

Cell viability was calculated relative to the negative control (untreated cells) according to the equation: Viability (%) = $(F_{sample}/F_{control}) \times 100$, where F is the fluorescence intensity (arbitrary units). Concentration–response curves were generated using GraphPad Prism version 11 (GraphPad Software, Boston, MA, USA). The half-maximal inhibitory concentration (IC_{50}), defined as the concentration required to reduce cell viability by 50%, was determined by nonlinear regression. Statistical differences among IC_{50} values were evaluated by one-way analysis of variance (ANOVA) followed by Tukey's multiple-comparisons test, with statistical significance set at $p < 0.05$.

3. Results

3.1. Extraction Yield and Chromatographic Fractionation

The chloroform extraction of the aerial parts of *P. angulata* (233 g) yielded 95.29 g of dry extract, corresponding to a yield of 40.89%.

Chromatographic partitioning of 3.00 g of E generated six fractions with different polarity profiles, among which the fraction eluted with hexane–ethyl acetate (6:4) (F) was selected for subsequent testing because its chromatographic profile was enriched in constituents of higher retention (39–40.7 min; Section 3.2); its yield was 6.22% (181.4 mg), calculated relative to the total mass recovered from the column.

3.2. Phytochemical Analysis (HPLC-UV)

The HPLC-UV chromatograms obtained for samples E and F at 230 nm showed complex chromatographic profiles with multiple peaks (Figure 1). The comparison focused on the retention-time range of 39–40.7 min, in which three prominent peaks were detected in both samples (Table 1). In sample E, these peaks occurred at retention times of 39.317, 39.508, and 40.650 min, with relative areas of 9.96%, 9.52%, and 10.68%, respectively. In sample F, the corresponding peaks occurred at 39.300, 39.500, and 40.617 min, with relative areas of 26.97%, 36.63%, and 18.98%, respectively.

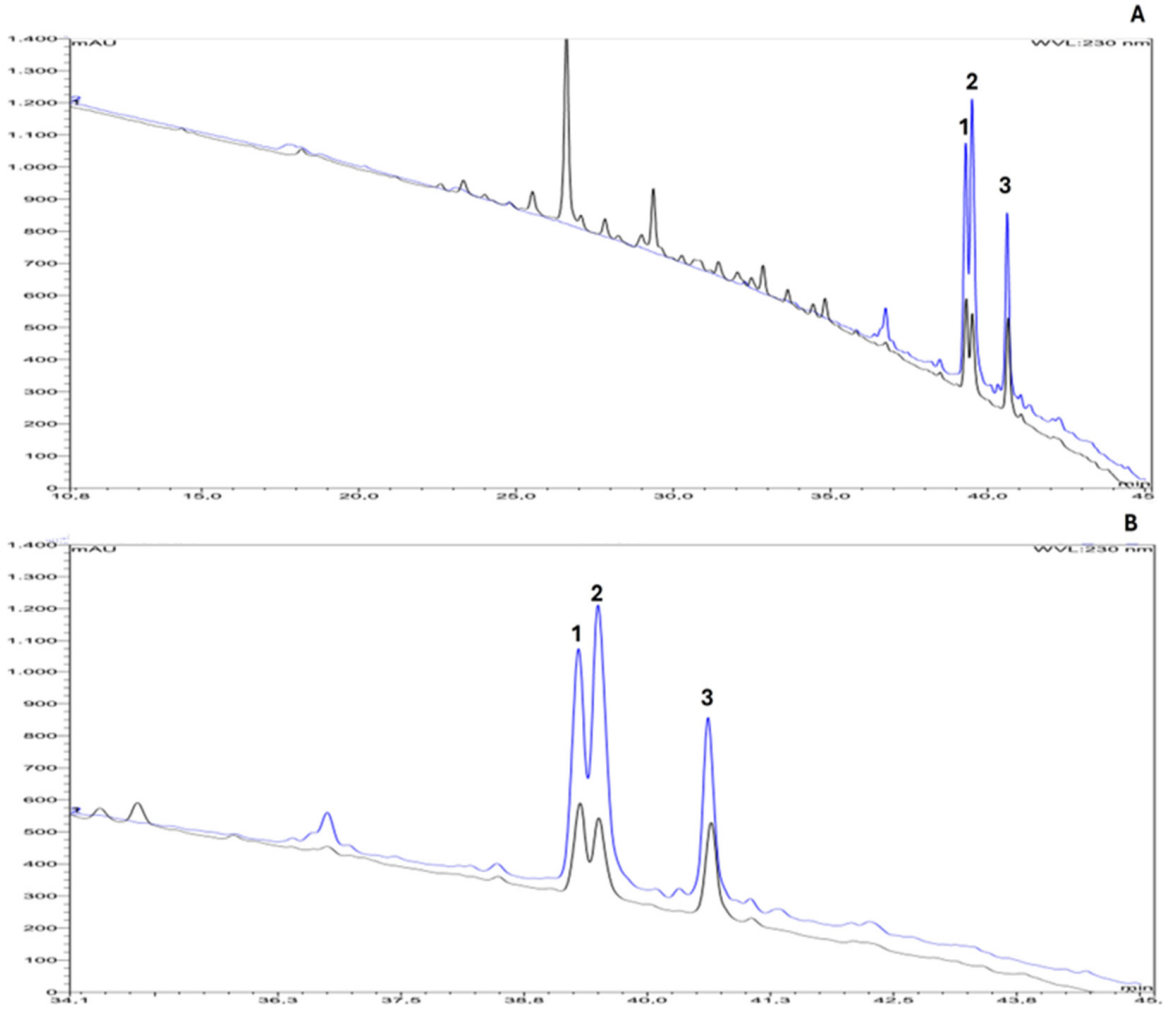

Figure 1. HPLC-UV chromatograms of extract E and fraction F recorded at 230 nm: (**A**) complete chromatographic profiles and (**B**) enlargement of the region between 33.9 and 45.2 min. The black and blue lines represent fraction F and extract E, respectively. Peaks 1–3 indicate the selected chromatographic peaks discussed in the text.

Table 1. Main chromatographic peaks of samples E and F obtained by HPLC-UV at 230.

Sample	λ (nm)	Peak N°.	Rt (min)	Area (mAU·min)	Relative Area (%)
E	230	1	39.317	39.43	9.96
	230	2	39.508	37.66	9.52
	230	3	40.650	42.25	10.68
F	230	1	39.300	111.32	26.97
	230	2	39.500	151.22	36.63
	230	3	40.617	78.36	18.98

λ: wavelength; Peak N°.: numbering corresponding to that shown in Figure 1; Rt: retention time; Area: peak integration; Relative area: percentage relative to the total area at 230 nm. Only the three selected peaks within the 39–40.7 min retention-time range are shown for each sample. The compounds were not chemically identified.

The similar retention times suggest that E and F may share constituents within this chromatographic region. However, the relative contribution of these peaks to the total chromatographic area differed between samples. The three peaks accounted for 30.16% of the total chromatographic area in E and 82.58% in F, corresponding to an approxi-

mately 2.74-fold higher relative contribution in F. This finding indicates that the selected chromatographic region accounts for a substantially greater proportion of the detected signal in F than in E, consistent with a change in the relative chromatographic profile following fractionation.

Under the analytical conditions used, the chromatographic profiles also differed in the distribution of detected peaks. F showed fewer detected peaks than E, suggesting a less complex detected chromatographic profile. Nevertheless, peak detection and relative peak areas depend on the analytical conditions and detector response and do not directly establish the absolute concentrations or identities of individual constituents.

Overall, the HPLC-UV results indicate differences in the chromatographic profiles of E and F, particularly in the relative contribution of the peaks detected between 39 and 40.7 min. These differences may be relevant to the distinct biological responses observed for the samples. However, because the compounds were not chemically identified, their individual contributions to the biological effects remain undetermined.

3.3. Antioxidant Activity Evaluation

The antioxidant activity of the samples was assessed using the DPPH assay, and EC_{50} values were determined by linear regression. Among the tested standards, gallic acid exhibited the highest activity (EC_{50} = 0.97 μg/mL), followed by ascorbic acid (2.49 μg/mL), quercetin (3.98 μg/mL), and rutin (26.76 μg/mL), supporting their use as reference compounds. Sample E showed an EC_{50} of 415.00 μg/mL, whereas sample F did not exhibit significant activity at the tested concentrations.

3.4. Nanoemulsion Characterization

The formulations NE-E, NE-F, and NE-B were evaluated for mean droplet diameter, polydispersity index (PDI), and zeta potential on days 1, 7, and 30 after preparation. The results are presented in Table 2. Droplet size showed statistically significant changes relative to Day 1 on Days 7 and 30 for all three formulations. PDI also varied significantly over time at most evaluated time points, except for NE-F on Day 30, which did not differ significantly from Day 1 (PDI ≈ 0.19).

Table 2. Mean droplet size, PDI, and zeta potential of the nanoemulsions on days 1, 7, and 30 (n = 3).

Formulation	Day	Size (nm)	PDI	Zeta Potential (mV)
NE-B	1	68.13 ± 0.57	0.28 ± 0.01	−13.4 ± 0.66
	7	59.04 ± 0.06 *	0.31 ± 0.01 *	−24.7 ± 0.76 *
	30	72.05 ± 0.35 *	0.18 ± 0.007 *	−26.8 ± 0.75 *
NE-E	1	40.09 ± 0.26	0.36 ± 0.012	−23.6 ± 1.42
	7	82.7 ± 0.54 *	0.20 ± 0.01 *	−28.5 ± 1.98
	30	78.5 ± 0.12 *	0.27 ± 0.023 *	−26.4 ± 1.65
NE-F	1	39.85 ± 0.19	0.19 ± 0.005	−17.3 ± 6.88
	7	55.2 ± 1.00 *	0.25 ± 0.01 *	−33.9 ± 0.64 *
	30	68.9 ± 0.14 *	0.187 ± 0.02	−26.3 ± 1.87 *

Data expressed as mean ± standard deviation (SD). Statistical differences were evaluated by two-way ANOVA followed by Dunnett's multiple-comparisons test, using Day 1 as the reference within each formulation. * indicates a statistically significant difference compared with Day 1 ($p < 0.05$).

Regarding zeta potential, NE-B and NE-F showed a statistically significant, more negative surface charge on Days 7 and 30 compared with Day 1. In contrast, NE-E showed

no statistically significant difference in zeta potential throughout the evaluated period, suggesting greater stability of this parameter specifically for this formulation.

Despite the statistically significant variations in droplet size and PDI over time, all three formulations remained within a droplet size range compatible with nanoemulsion systems (<300 nm) throughout the evaluated period [2,27].

3.5. Antimicrobial Activity Assessment

The antifungal activity results against the six microorganisms evaluated are summarized in Tables 3 and 4. Fraction F showed the lowest MIC values among the plant-derived samples and was active against all six microorganisms, with the lowest MIC against *M. canis* (0.07 mg/mL), three dilution steps (8-fold) below that of E (0.62 mg/mL). Among the dermatophytes, F was also active against *T. rubrum* (MIC = 0.31 mg/mL) and *T. mentagrophytes* (MIC = 0.62 mg/mL); among the yeasts, F showed a MIC of 1.25 mg/mL for all three species evaluated (*C. albicans*, *C. krusei*, and *C. parapsilosis*).

Table 3. Antifungal activity of the samples against dermatophytes evaluated (MIC and MFC, mg/mL).

Sample	*M. canis* MIC	*M. canis* MFC	*T. rubrum* MIC	*T. rubrum* MFC	*T. mentagrophytes* MIC	*T. mentagrophytes* MFC
E	0.62	5	2.5	2.5	>5	>5
F	0.07	0.31	0.31	0.31	0.62	0.62
NE-E	1.25	1.25	>1.25	>1.25	>1.25	>1.25
NE-F	0.31	0.31	0.62	0.62	1.25	1.25
NE-B	>1.25	>1.25	>1.25	>1.25	>1.25	>1.25
Ampho B (µg/mL)	0.31	0.31	0.15	0.15	<0.03	<0.03

MIC: Minimum Inhibitory Concentration; MFC: Minimum Fungicidal Concentration; NE-B: blank nanoemulsion, formulation control; Ampho B: amphotericin B (positive control). MIC values are expressed in mg/mL for the extracts, fractions, and nanoemulsions, and in µg/mL for amphotericin B. Values preceded by ">" indicate no activity at the highest concentration tested.

Table 4. Antifungal activity of the samples against the yeasts evaluated (MIC and MFC, mg/mL).

Sample	*C. albicans* MIC	*C. albicans* MFC	*C. krusei* MIC	*C. krusei* MFC	*C. parapsilosis* MIC	*C. parapsilosis* MFC
E	1.25	>5	2.5	2.5	2.5	>5
F	1.25	1.25	1.25	1.25	1.25	1.25
NE-E	>1.25	>1.25	>1.25	>1.25	>1.25	>1.25
NE-F	>1.25	>1.25	>1.25	>1.25	>1.25	>1.25
NE-B	>1.25	>1.25	>1.25	>1.25	>1.25	>1.25
Ampho B (µg/mL)	0.07	0.07	0.07	0.07	0.07	0.07

MIC: Minimum Inhibitory Concentration; MFC: Minimum Fungicidal Concentration; NE-B: blank nanoemulsion, formulation control; Ampho B: amphotericin B (positive control). MIC values are expressed in mg/mL for the extracts, fractions, and nanoemulsions, and in µg/mL for amphotericin B. Values preceded by ">" indicate no activity at the highest concentration tested.

Extract E showed lower antifungal potency than F against the three dermatophytes, with no detectable activity against *T. mentagrophytes* within the tested concentration range (MIC > 5 mg/mL). Against the yeasts, E showed modest activity, with MIC ranging from 1.25 to 2.5 mg/mL, depending on the species.

Following nanoemulsification, NE-F retained activity against all three dermatophytes tested, although with reduced potency relative to the non-formulated fraction—for in-

stance, the MIC against *M. canis* increased from 0.07 mg/mL (F) to 0.31 mg/mL (NE-F), an approximately 4-fold reduction in potency. In contrast, NE-F showed no detectable activity against any of the three *Candida* species within the tested concentration range (MIC > 1.25 mg/mL).

NE-E showed a more pronounced loss of activity relative to extract E, with no detectable activity against *T. rubrum*, *T. mentagrophytes*, or any of the three *Candida* species (MIC > 1.25 mg/mL), retaining activity only against *M. canis* (MIC = 1.25 mg/mL). The blank nanoemulsion (NE-B) showed no detectable antifungal activity against any of the six microorganisms evaluated within the tested concentration range, confirming that the formulation components alone did not contribute to the observed antifungal effects.

Amphotericin B, used as the positive control, showed MIC values in the μg/mL range for all six microorganisms.

3.6. Irritant Potential Assessment by HET-CAM

HET-CAM analysis showed that only the positive control (0.1 M NaOH) induced evident signs of irritation on the chorioallantoic membrane, with a mean irritation score (IS) greater than 20, classified as (+++) severely irritating. In the test groups—E, F, NE-E, NE-F, and NE-B—as well as in the negative control (0.9% NaCl), no vascular alterations were observed within 300 s. All samples presented an IS of 0.07 and were classified as (−) non-irritating (Table 5).

Table 5. Mean irritation score in the HET-CAM assay (*n* = 3).

	NaOH	NaCl	E	F	NE-B	NE-E	NE-F
Irritation Score	20.18 ± 0.10	0.07 ± 0.00	0.07 ± 0.00	0.07 ± 0.00	0.07 ± 0.00	0.07 ± 0.00	0.07 ± 0.00
HET CAM Score	+++	−	−	−	−	−	−

IS: irritation score. Classification: (−) no irritation; (+) slight; (++) moderate; (+++) severe.

These results indicate that none of the tested formulations caused irritation to the CAM, even after 5 min of exposure, reinforcing the preliminary safety profile of the nanoemulsions and their plant-based constituents (Figure 2).

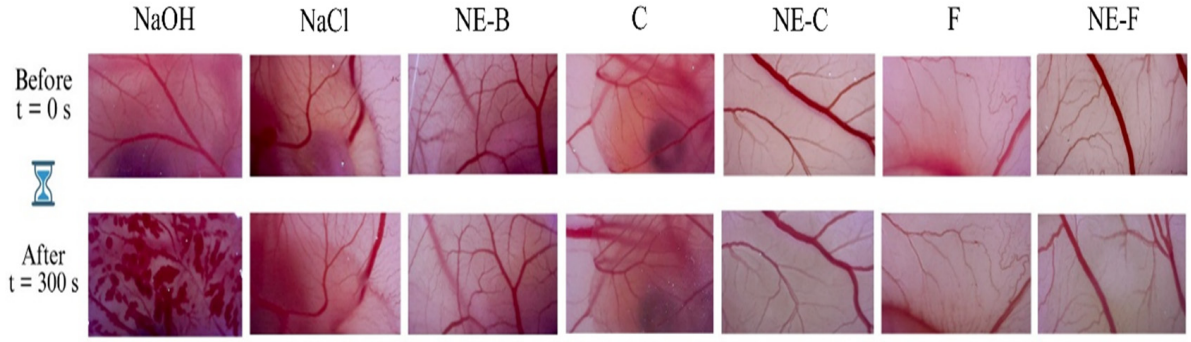

Figure 2. Representative images of the CAM before and after 300 s of sample application.

3.7. In Vitro Cytotoxicity Assessment

Cell viability in HaCaT keratinocytes was evaluated after 24 h of exposure to E, F, NE-E, NE-F, and NE-B, and IC_{50} values were determined by nonlinear regression (Table 6). NE-F showed the lowest IC_{50} (173.1 μg/mL), indicating the highest cytotoxic potency among the samples evaluated, followed by NE-E (199.2 μg/mL), E (233.3 μg/mL), F (262.8 μg/mL), and NE-B (335.0 μg/mL), which showed the lowest cytotoxic potency. Statistical analysis

confirmed that all five formulations differed significantly from one another ($p < 0.05$), as indicated by the distinct superscript letters in Table 6.

Table 6. Half-maximal inhibitory concentration (IC_{50}) of the samples in HaCaT keratinocytes.

Sample	IC_{50} (μg/mL)
E	233.3 [c]
F	262.8 [d]
NE-E	199.2 [b]
NE-F	173.1 [a]
NE-B	335.0 [e]

IC_{50}: concentration that reduces cell viability by 50%. Determined by resazurin-based fluorescence assay. NE-B: blank nanoemulsion; NE-E: nanoemulsion containing E; NE-F: nanoemulsion containing F. Different superscript letters indicate statistically significant differences between treatments according to Tukey's multiple-comparisons test ($p < 0.05$).

Notably, the nanoemulsified forms of both the extract and the fraction (NE-E and NE-F) showed lower IC_{50} values—and therefore significantly higher cytotoxic potency—than their respective non-formulated samples (E and F). This contrasts with the reduced antifungal potency observed for fraction F after nanoemulsification (Section 3.5). Thus, nanoemulsification increased cytotoxic potency while reducing antifungal potency, indicating that its effects differed between the two biological outcomes.

4. Discussion

The selection of chloroform as the extraction solvent was based on previous reports describing its effectiveness in obtaining physalins and related steroidal constituents from the aerial parts of *P. angulata* [6,7]. The solvent was removed by evaporation during extract processing (Section 2.1) and therefore was not intended to remain in the material incorporated into the final formulations. Nevertheless, considering the toxicity associated with chloroform and its limited relevance for cosmetic manufacturing at scale, future studies may investigate alternative, cosmetic-grade solvents capable of reproducing the extraction profile obtained in this work.

The high extraction yield obtained from the chloroform extraction of *P. angulata* aerial parts (E), together with the fatty consistency of the extract, is compatible with the co-extraction of lipophilic constituents of different chemical classes, such as cuticular waxes, pigments, and fatty acids, which may be extracted from plant material by solvents such as chloroform [14]. Although fraction F showed a lower overall yield, its chromatographic profile differed quantitatively from that of E. HPLC-UV analysis at 230 nm revealed that the three selected peaks within the 39–40.7 min retention-time range accounted for 30.16% of the total chromatographic area in E and 82.58% in F, corresponding to an approximately 2.74-fold higher relative contribution in F. This finding is consistent with a change in the relative chromatographic profile following fractionation and supports the selection of F for the subsequent biological assays. The detected constituents were not chemically identified, and their characterization remains an important direction for future studies. The DPPH assay demonstrated moderate antioxidant activity for extract E, while fraction F showed limited free radical scavenging capacity at the concentrations evaluated. This difference may be associated with variations in the chemical composition of the samples, including the relative distribution of lipophilic constituents. Such constituents may show different responses in hydrogen-donation assays such as DPPH [17,18]. Thus, fractionation may have altered the relative distribution of constituents contributing to the antioxidant activity observed in E. Recent studies reinforce the heterogeneity of antioxidant activity among

different *P. angulata* preparations. Untargeted chemical analysis by UHPLC-ESI-QTOF-MS has demonstrated substantial variation in antioxidant activity among extracts obtained from different plant organs (root, stem, leaves, calyx, and fruit), highlighting the influence of plant matrix and extraction method on the observed activity [28].

Beyond the phytochemical profile of the raw materials, the physicochemical behavior of the resulting nanoemulsions is a critical determinant of their performance as delivery systems. The physicochemical characterization of nanoemulsions revealed statistically significant variations in droplet size and PDI over time for all three formulations evaluated, which contrasts with the initial impression of physical stability attributed to these formulations. Nevertheless, all formulations remained within the droplet size range compatible with nanoemulsion systems (<300 nm) throughout the 30-day evaluation period, indicating that the observed variations, although statistically relevant, did not compromise the physical classification of the systems. A finding that deserves particular attention is the stability of the zeta potential of NE-E over time, with no significant difference relative to Day 1—in contrast to NE-B and NE-F, which showed significantly more negative surface charge on Days 7 and 30. This distinct behavior is consistent with reports that the composition of the internal oil phase is a key determinant of droplet size, PDI, and long-term stability in nanoemulsion systems [29], suggesting that the presence of extract E versus fraction F may differentially influence the electrostatic stability of the formulations. The PDI and zeta potential values obtained here are broadly consistent with those reported for other plant-derived nanoemulsions intended for topical use, such as flavonoid-loaded nanoemulsions with droplet size near 300 nm, PDI above 0.12, and zeta potential around −40 mV [27,30]—an aspect that may guide future studies on long-term stability optimization. Fraction F showed the lowest MIC values among the plant-derived samples, with activity against all six tested microorganisms and the lowest MIC against *M. canis* (0.07 mg/mL). This pattern—crude extract with modest activity and enriched fraction with lower MIC values—is consistent with previous reports involving *P. angulata* preparations, which described antimicrobial activity associated with physalin-rich fractions, although without detectable activity against *C. albicans* in the bioautography assay used [8]. Similarly, the crude extract of *P. angulata* has been shown to lack antifungal activity against *Candida* species (MIC > 2000 μg/mL), while an active fraction showed MIC values between 250 and 2000 μg/mL against the same yeast [31]. The results obtained here follow a comparable pattern: the activity of F against yeasts (MIC = 1.25 mg/mL) was consistently more modest than against dermatophytes, and this difference became more pronounced after nanoemulsification.

Nanoemulsification of F resulted in reduced antifungal potency against the three dermatophytes evaluated—approximately 4-fold against *M. canis* (MIC from 0.07 to 0.31 mg/mL)—and in complete loss of detectable activity against the three *Candida* species within the tested concentration range. This reduction may be associated with reduced availability of the free active compound following its incorporation into the nanoemulsion system, since parameters such as encapsulation efficiency and release rate—recognized as determinants of the biological performance of antifungal nanoformulations [32–34]—were not evaluated in this study. This limitation is common to several nanoformulation studies involving Brazilian natural products targeted at dermatophytes, in which characterizing the relationship between physicochemical parameters and biological performance remains a central methodological challenge—as illustrated by a recent study reporting low encapsulation efficiency (22.15%) for *Euphorbia tirucalli*-loaded polymeric nanoparticles evaluated against *T. rubrum* [35].

The comparison between F and NE-F should be interpreted considering the different vehicles used to evaluate the free fraction and the formulated system. In the biological

assays, F required solubilization in DMSO, an organic co-solvent used for in vitro testing but not intended for topical formulations. Nanoemulsification enabled the dispersion of this lipophilic fraction in an aqueous-based vehicle without an organic co-solvent [2,33,34]. The resulting formulation exhibited a droplet size below 70 nm, with PDI values ranging from approximately 0.19 to 0.25 over the 30-day evaluation period. Although these characteristics support the formation of a nanosized dispersion, statistically significant temporal variations in some physicochemical parameters should also be considered. Despite this formulation-related advantage, NE-F showed reduced antifungal potency against the three dermatophytes evaluated and no detectable activity against the three *Candida* species within the tested concentration range. Therefore, the present results demonstrate the feasibility of incorporating F into a nanoemulsion, but do not establish an improvement in antifungal efficacy. Further investigation of encapsulation efficiency, drug loading, and release profile is required to clarify the factors underlying the reduced activity and to guide subsequent formulation optimization [32–34]. The absence of detectable antifungal activity of the blank nanoemulsion (NE-B) against the microorganisms evaluated supports the interpretation that the activity observed with NE-F was associated with the plant-derived fraction rather than the formulation base. However, the present data do not establish whether the reduction in antifungal potency was related to encapsulation, the availability of active constituents, or their release from the droplets.

As a preliminary feasibility study focused on the incorporation of F into a nanoemulsion and the assessment of its biological activity, encapsulation efficiency, drug loading, and release profile were not determined. Accordingly, the concentrations used in the biological assays represent nominal values calculated from the amount of F added during formulation preparation (5 mg/g). Further characterization, together with the chemical identification of the active constituents, is needed to clarify the factors contributing to the reduced antifungal potency and to guide future formulation optimization [32–34].

The HET-CAM assay demonstrated that none of the tested samples induced detectable vascular irritation on the CAM within the evaluation period, with all formulations classified as non-irritating. In contrast, the positive control induced a severe irritation response, confirming assay sensitivity. The DMSO concentration used to solubilize E and F (1%) was defined beforehand based on prior laboratory standardization, so as not to compromise membrane viability and to ensure that the results reflected the response to the tested samples. These results constitute a preliminary safety indicator for the formulations, obtained from a single in vitro model; irritation scores obtained by HET-CAM have been reported to be consistently lower than corresponding in vivo scores, since the assay captures immediate, localized tissue damage rather than the broader inflammatory response evaluated in vivo [22]. Extrapolation to safety for topical use in humans therefore requires complementary assessments, including skin irritation and sensitization studies.

This combination of findings reinforces the importance of evaluating multiple safety parameters in a complementary manner, since the absence of irritation detected in the HET-CAM assay was not sufficient to anticipate the limited cellular safety margin revealed by the cytotoxicity assay. The cytotoxicity assessment in HaCaT keratinocytes revealed statistically significant differences among all five samples evaluated, with NE-F showing the highest cytotoxic potency (IC_{50} = 173.1 µg/mL) and NE-B the lowest (IC_{50} = 335.0 µg/mL). Notably, this pattern is the inverse of that observed for antifungal activity: while nanoemulsification reduced the antifungal potency of F (Section 3.5), it significantly increased its cytotoxic potency relative to the non-formulated fraction. This result indicates that the effects of nanoemulsification on bioactivity and on cytotoxicity do not follow the same direction, suggesting distinct mechanisms underlying each biological response. This divergence may be related to fundamental differences in membrane sterol composition between fungi and

mammalian cells—fungal membranes are structurally dependent on ergosterol, whereas mammalian membranes rely on cholesterol, a distinction that underlies the selectivity of several antifungal agents, including amphotericin B [36]—potentially resulting in differential interaction of the nanoemulsion system with fungal versus mammalian membranes.

This pattern is particularly relevant when considering the cellular safety margin of NE-F: for *M. canis*, the MIC (310 μg/mL) exceeded the IC_{50} (173.1 μg/mL), indicating that, under the conditions evaluated, the concentration required for antifungal activity exceeds the cytotoxic concentration in keratinocytes—a limited safety margin that must be considered in any future direction of this formulation toward topical application. The IC_{50} range observed here (173.1–335.0 μg/mL) is within the order of magnitude reported for other plant-derived nanoemulsions evaluated in HaCaT keratinocytes, even though direct numerical comparison is limited by differences in extract composition and testing conditions [30]. This finding reinforces the preliminary nature of the results presented here and the need for further formulation optimization—for example, through adjustments to encapsulation efficiency or the ratio between active compound and vehicle—before NE-F can be considered a viable candidate for topical development.

Together, these results demonstrate the in vitro antifungal potential of fraction F, particularly against dermatophytes, and its partial retention following incorporation into a nanoemulsion system, associated with physicochemical characteristics compatible with nanostructured systems and the absence of detectable irritant effects under the conditions evaluated. However, the limited cellular safety margin observed for NE-F, combined with the lack of confirmed chemical identification of the constituents responsible for the observed biological activity, reinforces the preliminary nature of these findings. Fraction F and its nanoemulsion therefore constitute a promising starting point for future investigation, contingent on formulation optimization—particularly encapsulation efficiency—and further chemical characterization of the active constituents, steps required before any assessment of suitability for cosmetic use.

5. Conclusions

This study demonstrated the in vitro antifungal potential of a chloroform extract (E) and a hexane–ethyl acetate fraction (F) obtained from *P. angulata*, with fraction F active against all six microorganisms evaluated (MIC of 0.07 mg/mL against *M. canis*, 0.31 and 0.62 mg/mL against *T. rubrum* and *T. mentagrophytes*, respectively, and 1.25 mg/mL against the *Candida* species). Fractionation increased the relative contribution of the three selected chromatographic peaks (39–40.7 min) from 30.16% in the crude extract to 82.58% in fraction F, corresponding to an approximately 2.74-fold higher relative contribution based on HPLC-UV peak areas at 230 nm.

Incorporation of F into a nanoemulsion system partially preserved this activity against the dermatophytes evaluated, although with reduced potency (4-fold increase in MIC against *M. canis*) and complete loss of detectable activity against the *Candida* species tested.

The nanoemulsions developed showed physicochemical characteristics compatible with nanostructured systems, with droplet sizes remaining below 100 nm throughout the 30-day evaluation period, despite statistically significant variations in some parameters over time. None of the formulations showed detectable irritant effects in the HET-CAM assay (IS = 0.07). However, cytotoxicity assessment revealed a limited cellular safety margin for NE-F, whose antifungal MIC against *M. canis* (310 μg/mL) exceeded its IC_{50} (173.1 μg/mL) in HaCaT keratinocytes—a finding that must be considered in any future direction for this formulation.

Unlike previous studies with *P. angulata*, which evaluated non-formulated extracts or fractions, this work combined the antifungal evaluation against dermatophytes and

Candida species with the incorporation of the fraction into a nanoemulsion and the assessment of its physicochemical stability, irritancy, and keratinocyte cytotoxicity. Together, these results reinforce the interest in fraction F as a plant-derived source of antifungal compounds, particularly against dermatophytes, and demonstrate the preliminary feasibility of its incorporation into a nanoemulsion system. Chemical identification of the constituents responsible for the observed activity, optimization of encapsulation efficiency, and complementary safety assessments remain necessary steps before any consideration of cosmetic application, constituting relevant directions for future investigations.

Author Contributions: Conceptualization, R.S. and R.C.L.R.P.; methodology, C.C.B.M., A.G.d.S., M.C., C.B.S., F.G.S., A.H.J. and A.M.; formal analysis, C.C.B.M., R.S., M.L.B.D., W.D.R., J.D.L., A.L.R.G., P.S.T.d.C., M.C., A.M. and R.C.L.R.P.; investigation, C.C.B.M., R.S., M.L.B.D., W.D.R., J.D.L., A.L.R.G. and P.S.T.d.C.; resources, R.C.L.R.P.; data curation, C.C.B.M. and R.C.L.R.P.; writing—original draft preparation, C.C.B.M. and R.C.L.R.P.; writing—review and editing, C.C.B.M., R.S. and R.C.L.R.P.; supervision and project administration, R.C.L.R.P.; funding acquisition, R.C.L.R.P. All authors have read and agreed to the published version of the manuscript.

Funding: Coordenação de Aperfeiçoamento de Pessoal de Nível Superior (CAPES)–Finance Code 001.

Institutional Review Board Statement: Not applicable.

Informed Consent Statement: Not applicable.

Data Availability Statement: The raw data supporting the conclusions of this article will be made available by the authors on request.

Acknowledgments: The authors express their gratitude to the School of Pharmaceutical Sciences of Araraquara (UNESP). During the preparation of this manuscript, the authors used ChatGPT-6.2 to assist with the translation and to improve the clarity and fluidity of the text. The authors have reviewed and edited all AI-generated content and take full responsibility for the final version and content of this publication.

Conflicts of Interest: The authors declare no conflicts of interest.

Abbreviations

The following abbreviations are used in this manuscript:

Ampho B	Amphotericin B
CLSI	Clinical and Laboratory Standards Institute
CAM	Chorioallantoic membrane
DLS	Zeta potential by dynamic light scattering
DMEM	Dulbecco's Modified Eagle Medium
DMSO	Dimethyl sulfoxide
DPPH	1,1-diffenil-2-picrilhydrazil
E	Chloroform extract of *P. angulata*
EC_{50}	Concentration required to scavenge or inhibit 50% of the free radical
F	Hexane–ethyl acetate (6:4) fraction of *P. angulata*
HaCaT	HaCaT immortalized human keratinocytes
HET-CAM assay	Hen's Egg Test–Chorioallantoic Membrane
HPLC	High-Performance Liquid Chromatography
IC_{50}	Concentration of a substance that causes 50% inhibition of cell viability
M. canis	*Microsporum canis*
MIC	Minimum Inhibitory Concentration
MFC	Minimum Fungicidal Concentration
NE-B	Blank nanoemulsion without active compounds
NE-E	Extract nanoemulsions
NE-F	Fraction nanoemulsion

P. angulata	*Physalis angulata*
PDI	Polydispersity index
RPMI-1640	Roswell Park Memorial Institute 1640 medium
SisGen	National System for Genetic Heritage and Associated Traditional Knowledge Management
SDA	Sabouraud Dextrose Agar
UNESP	São Paulo State University
UV	Ultraviolet light

References

1. McMullen, R.L.; Dell'Acqua, G. History of natural ingredients in cosmetics. *Cosmetics* **2023**, *10*, 71. [CrossRef]
2. Iskandar, B.; Liu, T.W.; Mei, H.C.; Kuo, I.C.; Surboyo, M.D.C.; Lin, H.M.; Lee, C.K. A comprehensive review of design, preparation, formulation, and characterization. *J. Food Drug Anal.* **2024**, *32*, 428–458. [CrossRef] [PubMed]
3. Bezerra, J.J.L.; Silva, V.B.; Dourado, D. Traditional use of medicinal plants in Brazil to treat mycosis. *J. Herb. Med.* **2024**, *48*, 100961. [CrossRef]
4. Havlickova, B.; Czaika, V.A.; Friedrich, M. Epidemiological trends in skin mycoses worldwide. *Mycoses* **2008**, *51*, 2–15. [CrossRef] [PubMed]
5. Novitasari, A.; Rohmawaty, E.; Rosdianto, A.M. *Physalis angulata* Linn. as a medicinal plant (Review). *Biomed. Rep.* **2024**, *20*, 47. [CrossRef] [PubMed]
6. Pietro, R.C.L.R.; Kashima, S.; Sato, D.N.; Januário, A.H.; França, S.C. In vitro antimycobacterial activities of *Physalis angulata* L. *Phytomedicine* **2000**, *7*, 335–338. [CrossRef] [PubMed]
7. Januário, A.H.; Filho, E.R.; Pietro, R.C.; Kashima, S.; Sato, D.N.; França, S.C. Antimycobacterial physalins from *Physalis angulata* L. (Solanaceae). *Phytother. Res.* **2002**, *16*, 445–448. [CrossRef] [PubMed]
8. Silva, M.T.G.; Simas, S.M.; Batista, T.G.F.M.; Cardarelli, P.; Tomassini, T. Studies on antimicrobial activity, in vitro, of *Physalis angulata* L. (Solanaceae) fraction and physalin B. *Mem. Inst. Oswaldo Cruz* **2005**, *100*, 779–782. [CrossRef] [PubMed]
9. Damu, A.G.; Kuo, P.C.; Su, C.R.; Kuo, T.H.; Chen, T.H.; Bastow, K.F.; Lee, K.H.; Wu, T.S. Isolation, structures, and structure–cytotoxic activity relationships of withanolides and physalins from *Physalis angulata*. *J. Nat. Prod.* **2007**, *70*, 1146–1152. [CrossRef] [PubMed]
10. Wu, J.; Zhao, J.; Zhang, T.; Gu, Y.; Khan, I.A.; Zou, Z.; Xu, Q. Naturally occurring physalins from the genus Physalis: A review. *Phytochemistry* **2021**, *191*, 112925. [CrossRef] [PubMed]
11. Pinto, N.B.; Morais, T.C.; Carvalho, K.M.B.; Silva, C.R.; Andrade, G.M.; Brito, G.A.C.; Veras, M.L.; Pessoa, O.D.L.; Rao, V.S.; Santos, F.A. Topical anti-inflammatory potential of physalin E from *Physalis angulata* on experimental dermatitis in mice. *Phytomedicine* **2010**, *17*, 740–743. [CrossRef] [PubMed]
12. Suwarsa, O.; Dharmadji, H.P.; Rohmawaty, E.; Mareta, S.; Gunawan, H.; Dwiyana, R.F.; Achdiat, P.A.; Sutedja, E.; Pangastuti, M. The efficacy of topical formulation containing ciplukan (*Physalis angulata* Linn.) in modulating interleukin-17 and interferon gamma expression in mice (*Mus musculus*) psoriasis model. *J. Exp. Pharmacol.* **2023**, *15*, 367–374. [CrossRef] [PubMed]
13. Nguyen, K.T.; Tran, L.H.; Nguyen, N.-V.T.; Duong, N.T.; Dai, X.-T.T.; Le, C.-T.T.; Nguyen, K.-N.H. New QuEChERS method for quantification of physalin B and D in *Physalis angulata* L. in Vietnam. *Pharmacia* **2022**, *69*, 883–890. [CrossRef]
14. Barthwal, R.; Mahar, R. Exploring the significance, extraction, and characterization of plant-derived secondary metabolites. *Metabolites* **2024**, *14*, 119. [CrossRef] [PubMed]
15. Hostettmann, K.; Hostettmann, M.; Marston, A. *Preparative Chromatography Techniques: Applications in Natural Product Isolation*; Springer: Berlin/Heidelberg, Germany, 1998.
16. Perez, N. Isolation and purification techniques in natural products chemistry. *J. Pharmacogn. Nat. Prod.* **2024**, *10*, 302.
17. Molyneux, P. The use of the stable free radical diphenylpicrylhydrazyl (DPPH) for estimating antioxidant activity. *Songklanakarin J. Sci. Technol.* **2004**, *26*, 211–219.
18. Gulcin, İ.; Alwasel, S.H. DPPH radical scavenging assay. *Processes* **2023**, *11*, 2248. [CrossRef]
19. Clinical and Laboratory Standards Institute. *Reference Method for Broth Dilution Antifungal Susceptibility Testing of Filamentous Fungi. M38*, 3rd ed.; CLSI: Wayne, PA, USA, 2017.
20. Clinical and Laboratory Standards Institute. *Reference Method for Broth Dilution Antifungal Susceptibility Testing of Yeasts. M27*, 4th ed.; CLSI: Wayne, PA, USA, 2017.
21. Herman, T.S.; da Silva Goersch, C.; Bocca, A.L.; Fernandes, L. Resazurin to determine the minimum inhibitory concentration on antifungal susceptibility assays for *Fonsecaea* sp. using a modified EUCAST protocol. *Braz. J. Microbiol.* **2024**, *55*, 1349–1357. [CrossRef] [PubMed]

22. Batista-Duharte, A.; Jorge Murillo, G.; Pérez, U.M.; Tur, E.N.; Portuondo, D.F.; Martínez, B.T.; Téllez-Martínez, D.; Betancourt, J.E.; Pérez, O. The Hen's egg test on chorioallantoic membrane. *Int. J. Toxicol.* **2016**, *35*, 627–633. [CrossRef] [PubMed]
23. Steiling, W.; Bracher, M.; Courtellemont, P.; de Silva, O. The HET–CAM, a useful in vitro assay for assessing the eye irritation properties of cosmetic formulations and ingredients. *Toxicol. Vitr.* **1999**, *13*, 375–384. [CrossRef] [PubMed]
24. Boukamp, P.; Petrussevska, R.T.; Breitkreutz, D.; Hornung, J.; Markham, A.; Fusenig, N.E. Normal keratinization in a spontaneously immortalized aneuploid human keratinocyte cell line. *J. Cell Biol.* **1988**, *106*, 761–771. [CrossRef] [PubMed]
25. O'Brien, J.; Wilson, I.; Orton, T.; Pognan, F. Investigation of the Alamar Blue (resazurin) fluorescent dye for the assessment of mammalian cell cytotoxicity. *Eur. J. Biochem.* **2000**, *267*, 5421–5426. [CrossRef] [PubMed]
26. Vieira-da-Silva, B.; Castanho, M.A.R.B. Resazurin Reduction-Based Assays. *Molecules* **2023**, *28*, 2283. [CrossRef] [PubMed]
27. Mukherjee, P.; Baruah, K.N. Characterization of Nanoemulsion: Particle Size, Polydispersity Index, Zeta Po-tential, Thermal Stability, and Kinetic Stability. In *Essential Oil Extraction from Food By-Products*; Srivastav, P.P., Srivastava, B., Karunanithi, S., Eds.; Methods and Protocols in Food Science; Humana: New York, NY, USA, 2025. [CrossRef]
28. Vargas-Arana, G.; Torres-Benítez, A.; Ortega-Valencia, J.E.; Merino-Zegarra, C.; Carranza-Rosales, P.; Simirgiotis, M.J. Untargeted chemical profile, antioxidant, and enzyme inhibition activity of *Physalis angulata* L. from the Peruvian Amazon. *Antioxidants* **2025**, *14*, 246. [CrossRef] [PubMed]
29. Algahtani, M.S.; Ahmad, M.Z.; Ahmad, J. Investigation of factors influencing formation of nanoemulsion by spontaneous emulsification. *Bioengineering* **2022**, *9*, 384. [CrossRef] [PubMed]
30. Balestrin, L.A.; Kreutz, T.; Fachel, F.N.S.; Bidone, J.; Gelsleichter, N.E.; Koester, L.S.; Bassani, V.L.; Braganhol, E.; Dora, C.L.; Teixeira, H.F. *Achyrocline satureioides* (Lam.) DC (Asteraceae) extract-loaded nanoemulsions. *Pharmaceutics* **2021**, *13*, 1241. [CrossRef] [PubMed]
31. Alencar, B.B.; Melo, M.L.F.R.; Cosme, W.Z.; Dias, M.H.F.; Medeiros, C.C.B.; Sorrechia, R.; Pietro, R.C.L.R.; Silva, F.G.; Andrade, E.; Silva, M.; et al. Red light-mediated enhancement of the antifungal activity of *Physalis angulata* against *Candida* species. *Photochem. Photobiol. B* **2026**, *275*, 113363. [CrossRef] [PubMed]
32. Chattha, G.M.; Andrades Cappellari, Y.L.; Beys-da-Silva, W.O.; Frank, L.A.; Santi, L. Nanoformulations of essential oils for the treatment of fungal diseases. *Arch. Microbiol.* **2026**, *208*, 280. [CrossRef] [PubMed]
33. Srivastava, R.; Rawat, A.K.; Mishra, M.; Patel, A.K. Advancements in nanotechnology for enhanced antifungal drug delivery. *Infect. Disord. Drug Targets* **2024**, *24*, e021123223053. [CrossRef] [PubMed]
34. Tarannum, N.; Pooja, K.; Jakhar, S.; Mavi, A. Nanoparticles assisted intra and transdermic delivery of antifungal ointment. *Discov. Nano* **2024**, *19*, 11. [CrossRef] [PubMed]
35. Heya, M.S.; Verde-Star, M.J.; Rivas-Morales, C.; García-Hernández, D.; Tijerina-Sáenz, A.; López-Cabanillas-Lomelí, M.; Álvarez-Román, R.; Galindo-Rodríguez, S.A. In vitro antifungal activity of polymeric nanoparticles loaded with *Euphorbia tirucalli* extract. *Braz. J. Biol.* **2024**, *84*, e275974. [CrossRef] [PubMed]
36. Gutierrez-Perez, C.; Cramer, R.A. Targeting fungal lipid synthesis for antifungal drug development and potentiation of contemporary antifungals. *npj Antimicrob. Resist.* **2025**, *3*, 27. [CrossRef] [PubMed]

Disclaimer/Publisher's Note: The statements, opinions and data contained in all publications are solely those of the individual author(s) and contributor(s) and not of MDPI and/or the editor(s). MDPI and/or the editor(s) disclaim responsibility for any injury to people or property resulting from any ideas, methods, instructions or products referred to in the content.